

# Jason Microwave Radiometer Assessment against DMSP-SSM/I and TRMM-TMI

Victor Zlotnicki  
Jet Propulsion Laboratory, California Institute of Technology  
vz@pacific.jpl.nasa.gov

Presented at  
Jason Science Working Team Meeting  
21-23 October 2002, New Orleans, LA, USA.

## INTRODUCTION

Vertically-integrated water vapor from the Jason Microwave Radiometer, as reprocessed using the algorithm described in Ruf and Brown (19 July 2002 and 5 Aug 2002), has been compared to the same quantity estimated by Wentz et al (2002; Remote Sensing Systems, RSS, at [www.ssmi.com](http://www.ssmi.com)) from the three Special Sensor Microwave/Imager (SSM/I) instruments aboard the Defense Meteorological Satellite Program (DMSP) satellites F13, 14, and 15, and by the TRMM Microwave Imager (TMI) instrument flown aboard the Tropical Rainfall Mapping Mission (TRMM) satellite.

There are several differences between JMR and the other instruments that must be taken into account. most crucial are their different sampling patterns. JMR is a nadir-looking radiometer at 18.7, 23.8 and 34.0 GHz, in an orbit with an inclination of  $\sim 66.0^\circ$  and a period of  $\sim 112$  min. The SSM/I instruments are scanning radiometers at 19.35, 22.235, 37, and 85.5 GHz. Their DMSP satellites are in sun-synchronous, near-polar, orbits with an inclination of  $98.8^\circ$  (but local times of 6:15, 8:21, and 9:31). TMI is similar to SSM/I but with an additional frequency (10.7, 19.4, 21.3, 37, 85.5 GHz). Its TRMM satellite has an inclination of  $\sim 35^\circ$ , and a short period ( $\sim 91$ min) since it flies at a height of  $\sim 402$ km, about  $\frac{1}{2}$  the DMSP height and less than  $\sim \frac{1}{3}$  the Jason height (this also gives TMI finer spatial resolution).

The computations this author performed with the pre-launch Jason algorithms (presented at the June 2002 Jason Meeting in Biarritz, France) showed that the main features of JMR behaviour with the older algorithm were cleanly retrieved from this computation, including a weakly scale-dependent bias (as well as the yaw-dependence of TMR).

## DATA COVERAGE and SPACE-TIME SAMPLING

JMR data for cycles 17 to 27 were used (2002-06-22 to 2002-10-09). For cycles 17-22 the IGDR data were combined with the correction files (eg, JMR\_REPROCESS\_018.001) prepared by Shailen Desai, so they would have the same calibration that became incorporated into the Jason standard processing starting with cycle 23.

All the SSM/I data used are RSS's version 5 (August 2002). The TMI are RSS's version 3 (March 2002)

A 'matched pair' is defined where a JMR observation is within 1 hr of either SSM/I or TMI, and when the location of the Jason IGDR point is inside the 1/4° SSM/I or TMI cell (in Wentz's gridded product) . This produces a spatially varying sampling pattern with the SSM/Is, where only certain latitudes are sampled during any 10 day period. Both time series averaged over 1 day and the whole globe, and maps of 10-day spatial patterns are presented. Figures 1 and 2 illustrate the spatial sampling pattern.

The only Flag used for JMR is the surface type flag, set to 0 (ocean). The Flags used for SSM/I and TMI are scaled values up to 250, indicating clear ocean returns, uncontaminated by ice or land.

For the cycles used, these were the numbers of matched points:

CYCLE	# IGDR POINTS	# MATCHED PAIRS SSM/I		# MATCHED PAIRS TM/I	
17	534,447	53,841	10.1%	29,859	5.6%
18	542,559	23,314	4.3%	26,208	4.8%
19	550,997	88,619	16.1%	29,529	5.4%
20	553,032	168,131	30.4%	32,474	5.9%
21	524,080	230,840	44.0%	26,850	5.1%
22	549,830	155,956	28.4%	27,468	5.0%
23	561,153	71,676	12.8%	45,964	8.2%
24	561,152	49,235	8.8%	55,894	10.0%
25	562,164	185,794	33.0%	32,966	5.9%
26	556,280	352,154	63.3%	29,320	5.3%
27(partial)	253,251	109,357	43.2%	16,865	6.7%

There is an ~60-day cycle in the coverage of matched JMR – SSM/I because SSM/I is sun-synchronous, and the Jason orbit plane has an approximate 60 day periodicity with respect to the SUN.

FIGURE 1

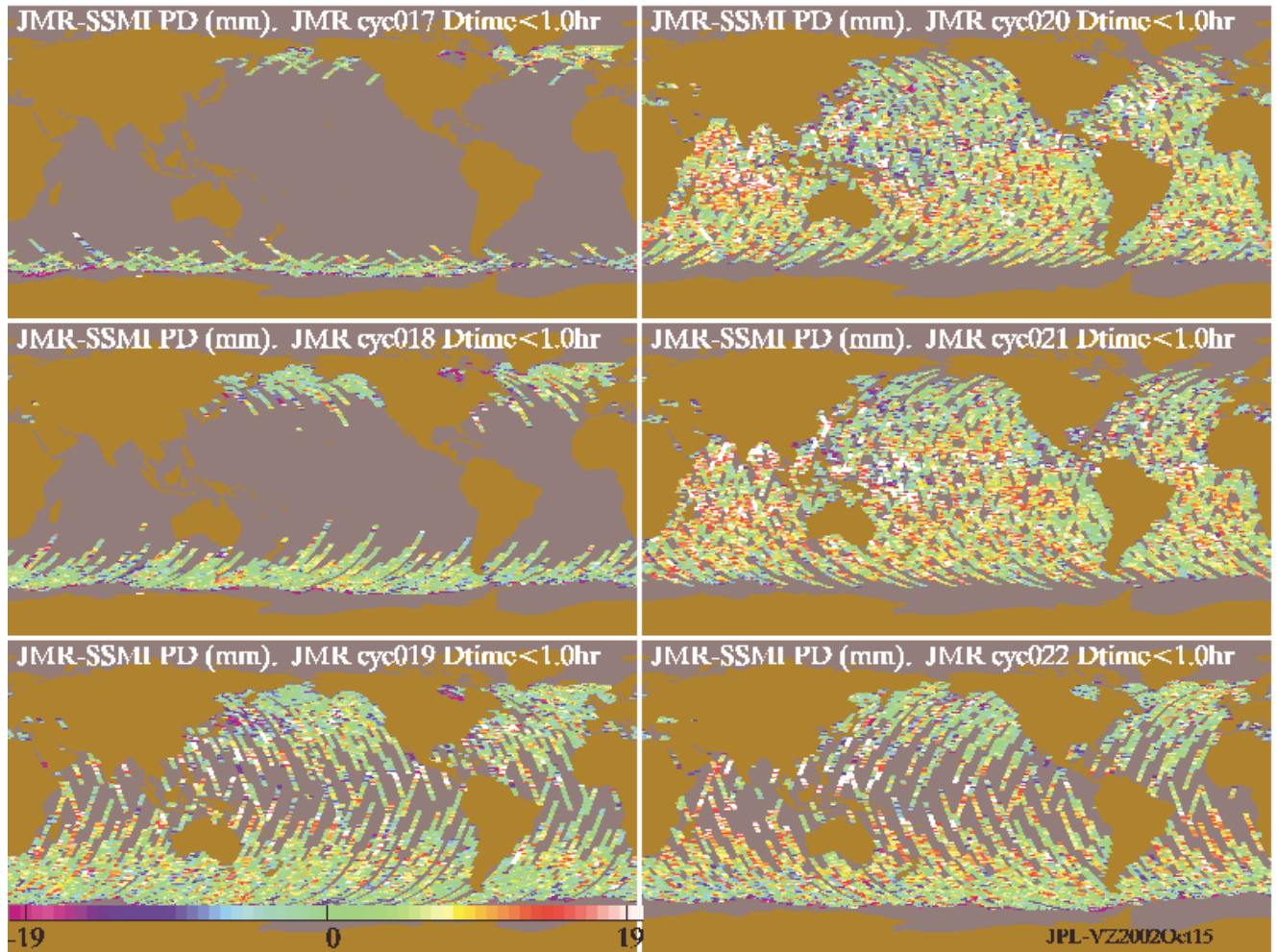
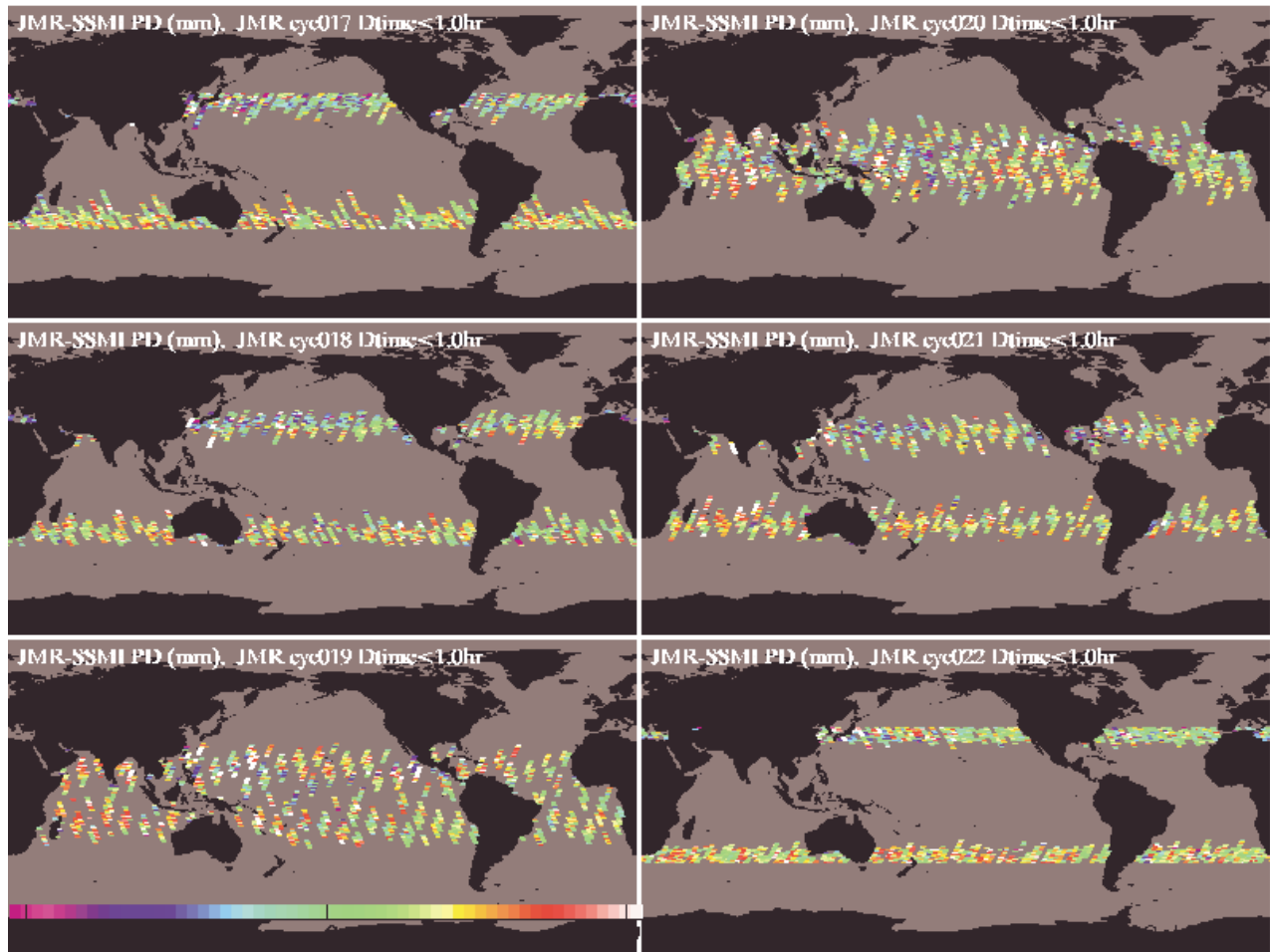


FIGURE 2



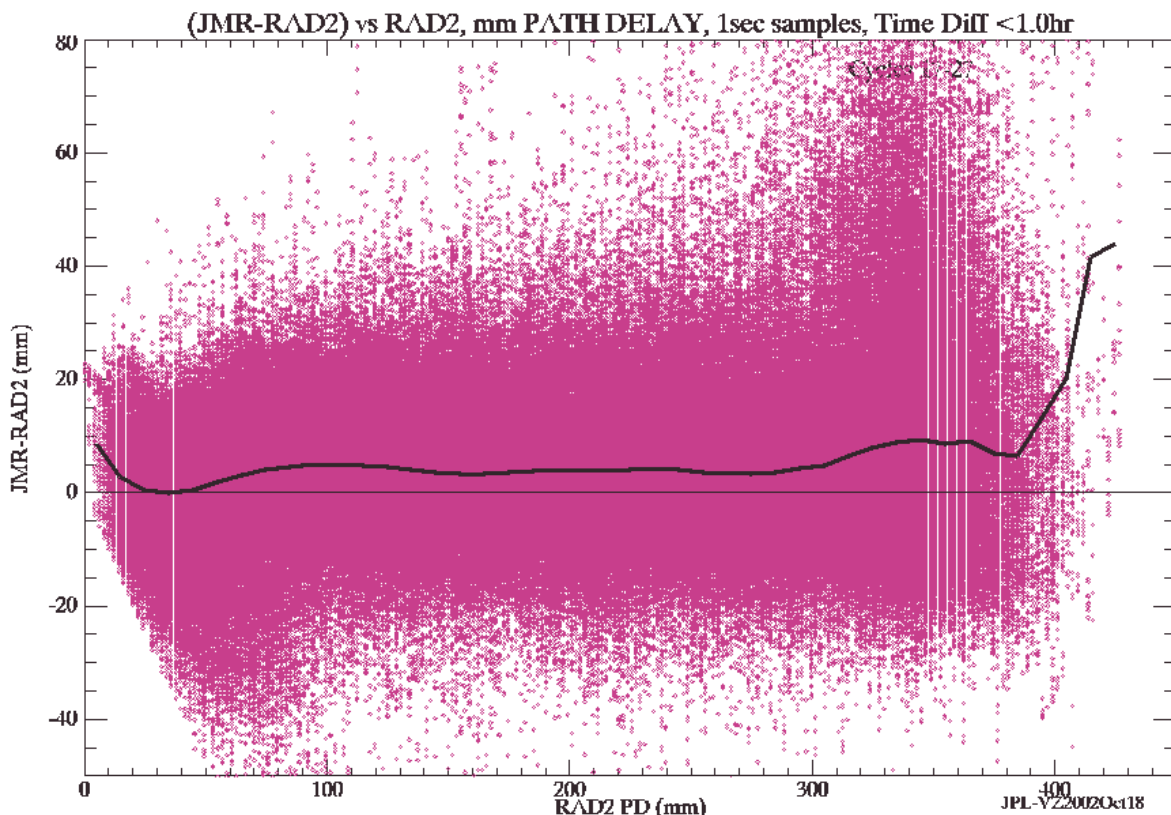
## SCALE-DEPENDENT DIFFERENCES

One key question addressed here is whether there is any suggestion of a scale-dependent error in the difference between JMR and the other radiometers.

To address that, Figure 3 shows the difference JMR-SSM/I in terms of radar Path Delay (PD), the quantity used to correct the altimeter measurement. The SSM/I and TMI datasets used here only provide the vertically-integrated water vapor (WV, in mm of precipitable water), hence it is necessary to convert these to PD. The algorithm used in Keihm et al (1998) is also used here, a cubic polynomial in WV.

Each purple dot in Figure 3a corresponds to one 1-sec Jason sample; the black line is an average of the difference in bins of SSM/I PD whose width is 5 mm PD. This plot suggests a bias of ~ 5 mm PD, which increased to about 10 mm PD at PD > 300mm and < 400mm (there are insufficient data for PD > 400mm, so the increase there is statistically unreliable).

FIGURE 3a



However, the conversion of WV to PD may cause this effect. Since the Jason IGDR includes both the WV and PD retrievals from JMR, Fig. 3b shows the equivalent plot in terms of WV. Because the difference curve over the range 0 to 64 mm WV is between 0 and 1 mm WV (~ 0 to

6.25 mm PD), one can conclude that to  $\pm 3$  mm PD there is no scale-dependent difference between JMR and SSM/I. The binned PD and WV curves are replotted in Fig 4.

FIGURE 3b

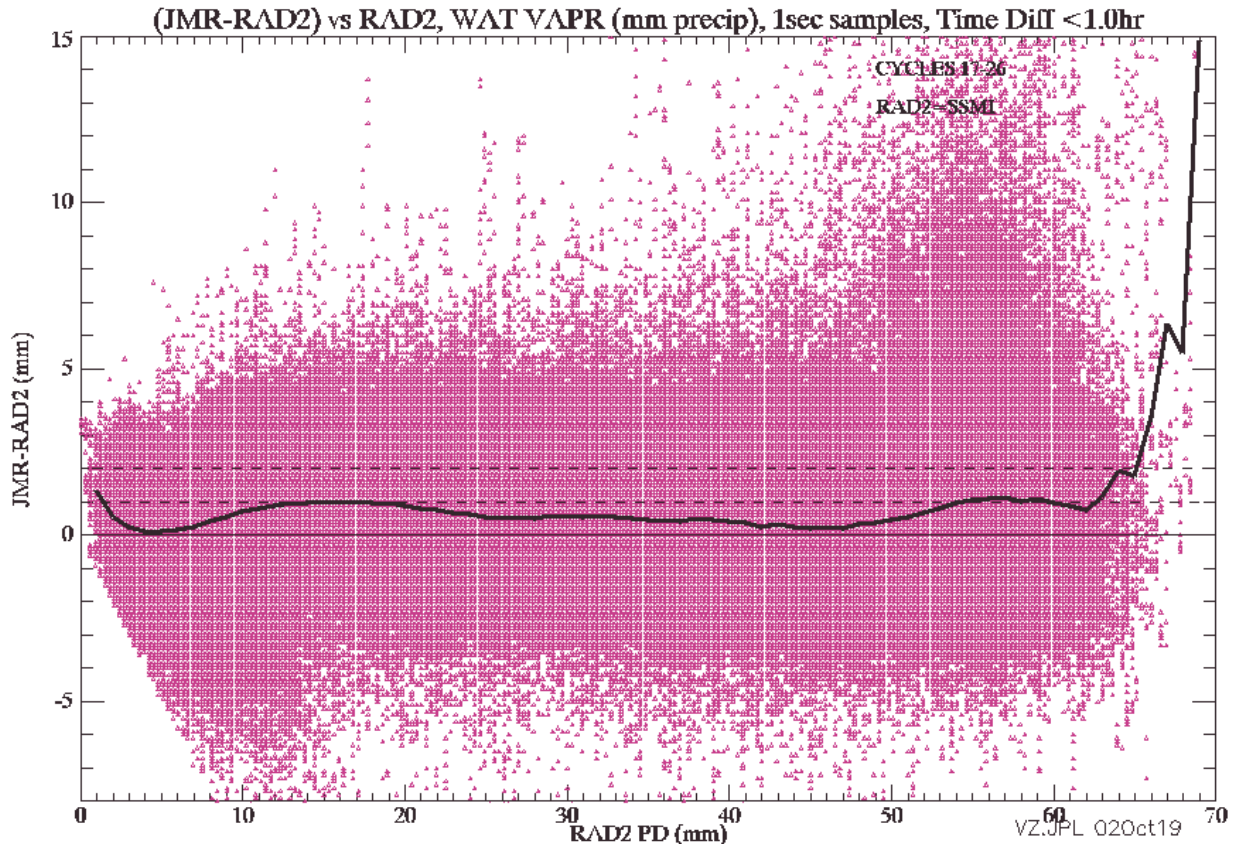


FIGURE 4

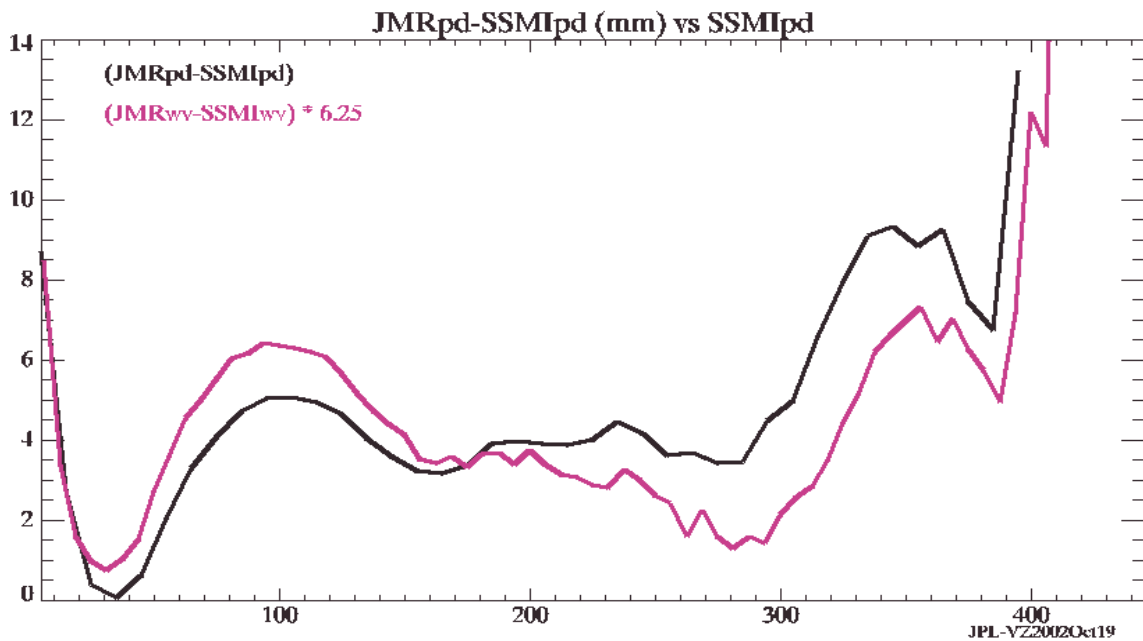
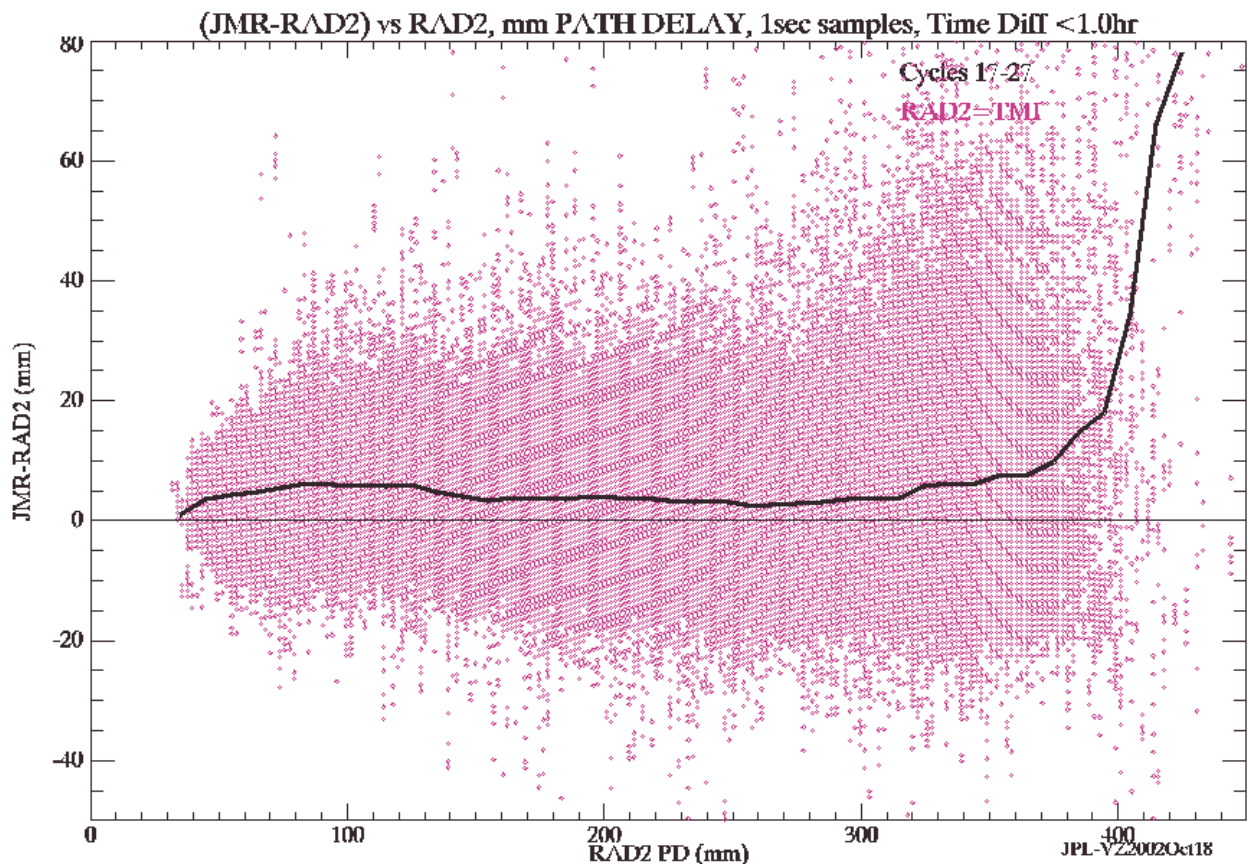


FIGURE 5



The JMR-TMI differences in Fig 5 are consistent with the JMR-SSMI differences. Hence, a similar conclusion: the absence of a scale-dependent discrepancy, follows from this comparison.

## TIME VARIATION

A surprising feature of TMR, the radiometer aboard the Topex/Poseidon satellite, was discovered early in 2002 by Don Chambers (U. Texas) in comparing JMR and TMR: a systematic 'jump' of ~ 5 mm every few weeks. Further work by several authors confirmed the presence of those features throughout the T/P mission, clearly visible in brightness temperatures (Tb) for the 3 frequencies, associated them with changes from yaw-fixed to yaw-sinusoidal steering (or viceversa), and further related them to insufficiently modelled internal temperatures. Brown, Ruf and Keihm (note dated 8 August 2002) then produced an algorithm to correct for these. A much weaker jump was also identified in JMR PD, because the effects on brightness temperatures (Tb) tended to cancel rather, and the corrections of Ruf and Brown (19 July 2002 and 5 Aug 2002) addressed this topic.

To assess whether significant time-dependent 'jumps' are visible in JMR-SSM/I or JMR-TMI, figures 6 and 7 show these daily-averaged differences versus time. The upper panel in each figure gives an idea of the range of daily-averaged PD sampled on that day by the *matched* pairs. Unfortunately, these range from < 80mm to > 180 mm for JMR-SSM/I and from 150 to 270 mm PD for JMR-TMI. The middle curve is the essential one, the difference in PD. It shows an ~5 mm bias in JMR-TMI, but in JMR-SSMI the bias only shows up when higher values of PD are sampled. As discussed above, these are due to the algorithm used to convert WV to PD, not to JMR itself.

Because the jumps in JMR-TMI do not correlate with those in JMR-SSM/I, and the number of points in JMR-TMI is much lower, we conclude that at this level of detection (2-3mm PD) there are no significant 'jumps' in the difference. (The JMR-SSM/I for Jason cycle 27 is due to the use of interim SSM/I data, which are replaced a few weeks later by the final version used for cycles 26 and earlier).



FIGURE 6

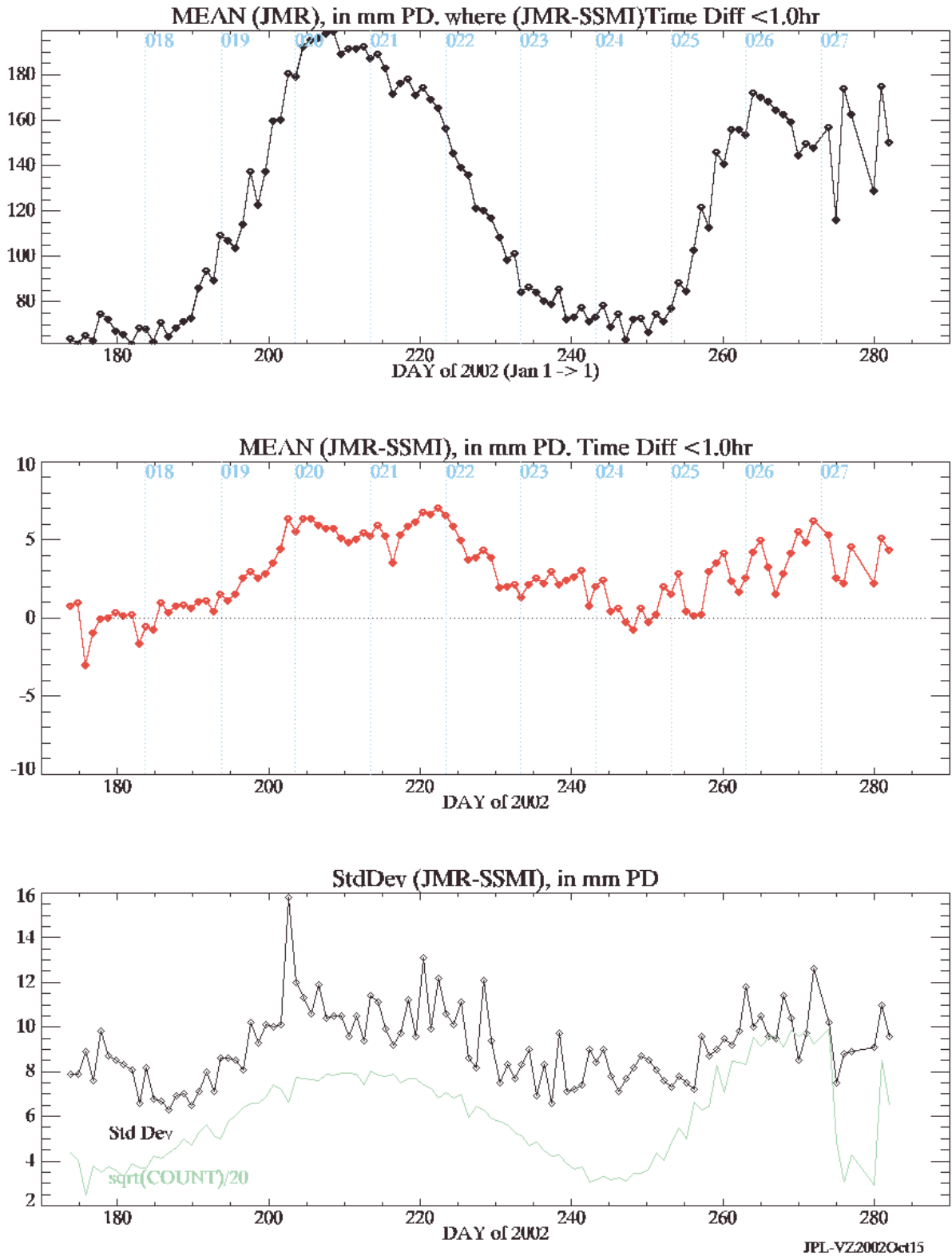
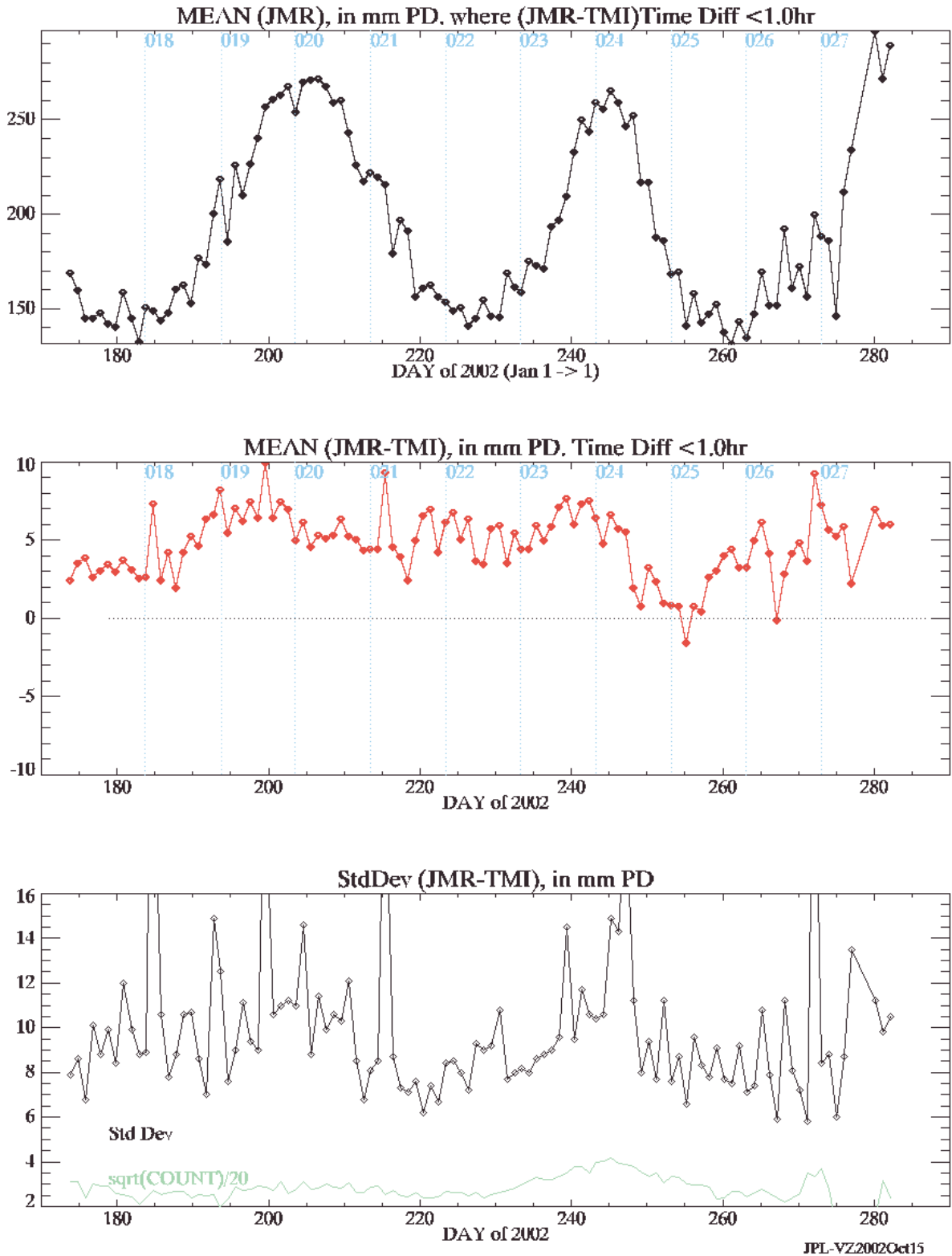


FIGURE 7



## OUTLIERS

All the JMR data used here were edited only using the radiometer surface flag (set to 0=oceans). Figures 8 and 9 show the location of PD values that are suspiciously large (although not necessarily wrong) for cycles 17 to 27. Just as there are values of PD with the wrong sign (equivalent to negative concentrations of water vapor) due to instrumental noise, there are a few unreasonable large values of PD (eg, 987 or 822 mm). A reasonable cutoff should be chosen to avoid contaminating the sea surface heights with uncertainties of several cm in high WV regions.

FIGURE 8

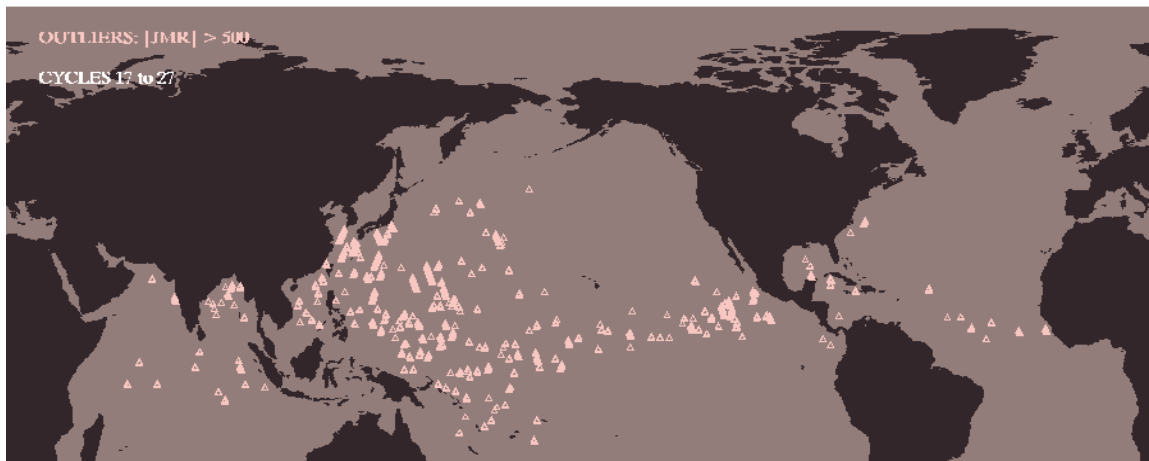


FIGURE 9



The total number of these outliers is below 0.1%, as shown in the table below

	MIN	MAX	>0mm	>500mm	>650mm
	-- (mmPD) --		----- (count) -----		
017	0	701	534447	266	26
018	0	795	542559	437	67
019	0	701	524080	318	18
020	-1	690	550997	104	5
021	-1	719	553032	238	16
022	0	822	549830	303	22
023	-36	987	561153	372	42
024	-43	714	561152	215	20
025	-20	659	562164	108	2
026	-29	768	556280	145	10
027	-24	756	253251	73	5(incomplete data)

### JMR compared to TMR

FIGURE 10

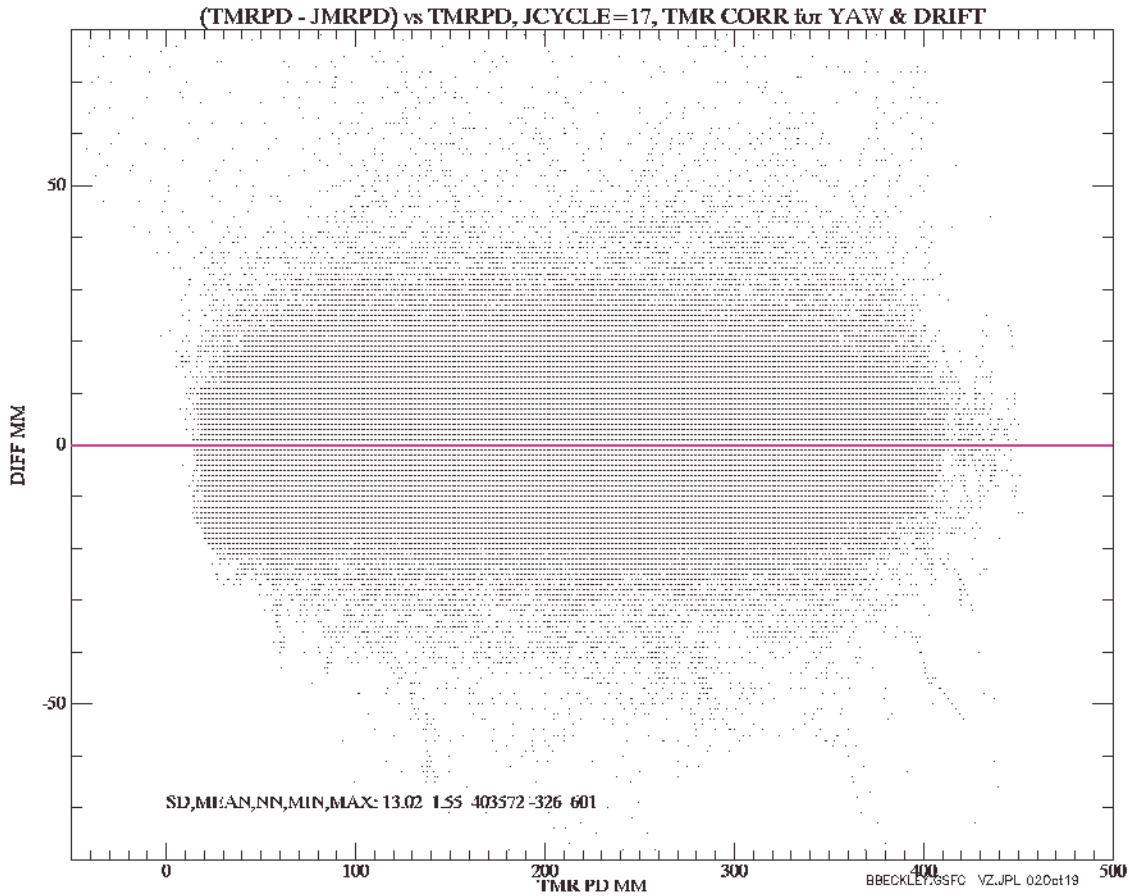


Figure 10 compares TMR PD and JMR PD during cycle 17. There is no significant scale-dependency or bias (the average difference is 1.5 mm; the std. dev is 13 mm). In a sense, this is not surprising because TMR was empirically adjusted to overcome the yaw-dependence, and JMR was adjusted to the corrected TMR. However, the data used by Ruf and collaborators to perform those adjustments did not include cycle 17, hence this is very reassuring.

## CONCLUSIONS.

The comparisons between JMR (as corrected after Jason cycle 23) and the SSM/I radiometers aboard three different DMSP satellites, and the TMI radiometer aboard TRM show no scale-dependent difference and no time-dependent jumps, at the +/- 2 to 3 mm PD level.

There is still an ~ 60 day periodicity to these differences with 5 mm range. This may be due to the sampling pattern of the matched points, or to a yaw-dependence in JMR.

The algorithm used above to convert water vapor to path delay would benefit from some refinement in the region  $PD > 300$  mm, as evidenced in the discrepancy between PD comparison against the WV comparison (see Appendix 1 for one such revision).

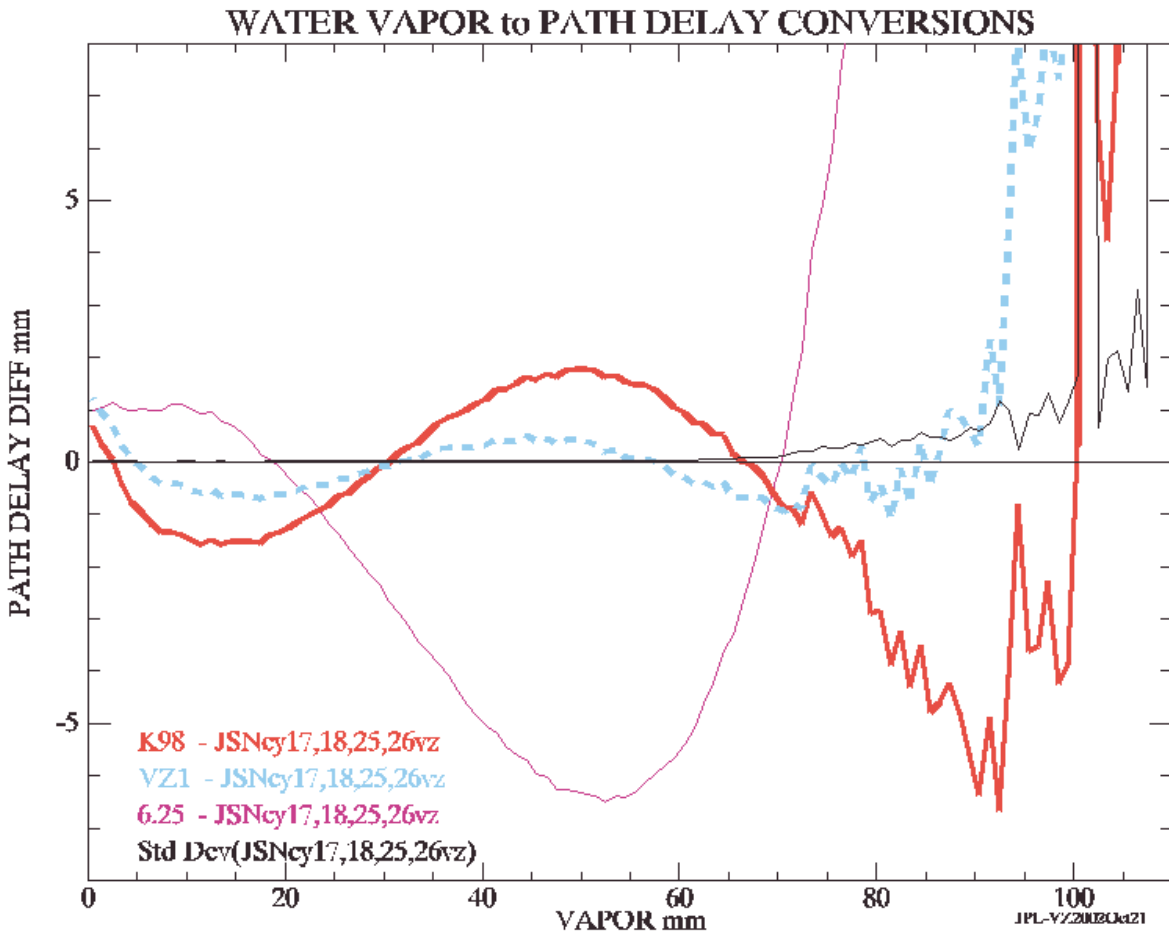
There is a need to guide users of the GDR on how to edit out unreasonably large values of PD. This would eliminate no more than 10 to 20 points per cycle.

The JMR cycle 17 comparison to TMR, with the yaw-dependence corrected, shows that both instruments are stable, and that the corrections to both are working properly, at the 1-2 mm PD level.

APPENDIX : REVISED WATER VAPOR TO PATH DELAY CONVERSION

Since the Jason IGDR provides both vapor (WV) and path delay (PD) fields, it is a simple matter to estimate a relationship from this dataset. On a plot of PD against WV, all such estimates are minute departures from a simple line with slope 6.25 (mmPD/mmWV). To highlight those departures, Fig. A1 shows the DIFFERENCES between three polynomial approximations and a non-parametric estimate, whereby the PD data for cycles 17,18,25,26 are averaged in bins whose width is 1 mmWV.

FIGURE A1



The thin purple curve shows the difference between 6.25\*WV and the Jason data. The thick red curve is the difference between the Keihm 98 algorithm used throughout this analysis and Jason data. The dashed blue curve is a cubic polynomial approximation to the Jason data in the range [0,90]mmWV range ([0,560]mmWV). The thin jagged black curve (indistinguishable from zero at WV <65mmWV) is the standard error of the Jason data in each bin. Notice that even this simple 'new' polynomial approximation is within 1 mm of the Jason data in the range [50-90] mmWV ([312-560]mmPD),

$$PD(mm)=a_0+a_1*WV+a_2*WV^2+a_3*WV^3$$

$$a_0=-0.44, a_1= 6.65341, a_2=-0.0232491, a_3= 2.53049e-4$$

NOTE added after the meeting: During the meeting, Steve Keihm explained the reason for the red curve above to be different from zero. The Jason GDR algorithms derive Path Delay (PD), not vapor (WV). The WV in the I/GDR is derived from the PD in the I/GDR by an approximate inverse of the K98 algorithm used here to convert SSM/I and TMI WV to PD. However, the inverse PD to WV conversion is not the exact inverse of the cubic polynomial in K98, rather it is a cubic polynomial fit to the same radiosonde data used to compute K98, using PD as the independent variable.